Arabian Journal for Science and Engineering (2018) 43:3557–3564
https://doi.org/10.1007/s13369-017-3028-7

RESEARCH ARTICLE - CHEMISTRY

# Hydrogen Sulfide Removal from Copper Smelting Contaminated Acid Using Rotating Packed Bed

Shiwei Li[1,2,3] · Xiaopeng Ren[1,2,3] · Chandrasekar Srinivasakannan[4] · Junwen Zhou[1,2,3] · Libo Zhang[1,2,3] · Jinhui Peng[1,2,3] · Weiheng Chen[1,2,3] · Jiannan Pei[1,2,3]

Received: 14 March 2017 / Accepted: 5 December 2017 / Published online: 20 December 2017


**Abstract**
The removal of $H_2S$ from copper smelting contaminated acid using sodium hydroxide (NaOH) as absorbent was investigated in a RPB reactor. The influences of operating parameters were assessed on the removal efficiency of $H_2S$ ($E$) and overall volumetric gas side mass transfer coefficient ($K_Ga$). The results illustrate that $E$ and $K_Ga$ increased with increase in high gravity factor, flow rate and concentration of sodium hydroxide while decreased with increase in mass concentration of $H_2S$ in feed gas. With increase in $H_2S$ gas flow rate, $E$ was found to decrease while $K_Ga$ was found to increase. The increase in the temperature of absorption did not show any significant effect on $E$ and $K_Ga$. The $K_Ga$ of the rotating packed bed reactor was about 30 times higher than the conventional packed bed at similar gas liquid throughputs. The superior performance of RBP certainly demands further investigation, process development, scale-up for economical commercial adoption.

**Keywords** Copper smelting contaminated acid · $H_2S$ · Sodium hydroxide solution · High gravity · Rotating packed bed

## 1 Introduction

The large quantities of sulfur dioxide in the smoke and vapor exhaust from copper smelting process are normally used for acid production. Gas washing is necessary before acid-making step which generates acid wastewater. Due to its high acidity, smelting enterprises generally refer it as "contaminated acid". The contaminated acid contains high concentration of fluorine, chlorine, arsenic and copper, zinc, lead, cadmium and other metals. The sulfide precipitation method has widely been used in treatment of contaminated acid due to high-efficiency and simplicity of operation. The sulfide precipitation process unfortunately generates significant quantities of $H_2S$ as byproduct, due to the reaction of sodium sulfide with sulfuric acid [1]. Generation of $H_2S$ is a serious HSE issue, and hence it is imperative to properly handle and treat $H_2S$, satisfying safety/environmental regulations.

Separation of $H_2S$ from mixture of gas streams also owes its relevance to gas processing and petroleum refining operations. Natural gas consists of large proportion of $H_2S$ while the liquid crude contains sulfur attached to hydrocarbons in various forms. The hydro-treating operations in the petroleum refineries convert sulfur to $H_2S$, while the gas processing industries separate $H_2S$ from the hydrocarbons. Handling $H_2S$ is of serious HSE concern as it is an extremely toxic gas even at very low concentrations. Different technologies are utilized for separation of $H_2S$ of which amine absorption using mono-, di- or tri-ethanolamines is considered cost effective and adopted widely in gas processing industries. Additionally separation of $H_2S$ is also effected through absorption with NaOH, with reference to the electrochemical conversion of $Na_2S$ to elemental sulfur [2–6]. In the alkali absorption process, $H_2S$ would react

✉ Xiaopeng Ren
1158767359@qq.com

Shiwei Li
lishiweikmust@163.com

Chandrasekar Srinivasakannan
csrinivasakannan@pi.ac.ae

1 State Key Laboratory of Complex Nonferrous Metal Resources Clean Utilization, Kunming University of Science and Technology, Kunming 650093, Yunnan, China

2 Yunnan Provincial Key Laboratory of Intensification Metallurgy, Kunming 650093, Yunnan, China

3 National Local Joint Laboratory of Engineering Application of Microwave Energy and Equipment Technology, Kunming 650093, Yunnan, China

4 Chemical Engineering Department, The Petroleum Institute, Khalifa University of Science and Technology, 2533, Abu Dhabi, UAE

with the NaOH to produce the $Na_2S$, which precipitate as sulfide utilizing the contaminated acid. Alkali absorption process can either be carried out in a packed tower or a plate tower. The effectiveness of gas liquid absorption process is governed by the solubility and the kinetics of transfer. The economics of gas liquid separation in turn depends on these two factors. A faster transfer rates can significantly alter the economics as the column size can be considerably reduced. So as to increase the transfer rates recent process intensification efforts include utilization of as membrane contactors, microchannel reactors and rotating packed beds [7–12].

The rotating packed bed (RPB) reactor rotates at high speed with doughnut-shaped packing driven by a motor, which accounts for increased specific surface area of the liquid [13–16]. The mass transfer rates were reported to improve up to 3 orders of magnitudes as compared to conventional gas liquid absorption operations in packed towers. Recently, RPB has been increasingly tested for its application for distillation [17], VOCs absorption [18], $CO_2$absorption [19], $O_3$absorption [20], ozonation[21], reactive precipitation [22], and stripping [23].

The present work attempts to separate $H_2S$ produced from copper smelting process by sodium hydroxide (NaOH) solution utilizing a RPB reactor. The influences of operating parameters on the removal efficiency of $H_2S$ ($E$) and overall volumetric gas side mass transfer coefficient ($K_Ga$) were estimated, so as to assess its effectiveness in comparison with conventional methods.

## 2 Experimental Section

### 2.1 Materials and Setup

The $H_2S$ used in experiments was provided by Yunnan Copper (Group) Co., LTD. The sodium hydroxide solution was purchased from Jilantai Chlor-Alkali Chemical Co., LTD.

Figure 1 is the schematic of the experimental setup for hydrogen sulfide removal from copper smelting acid gases using high gravity method. Its major components include an RPB, a contaminated acid tank, a blower, a drying system, a liquid feed pump, a liquid heater, two $H_2S$ analyzer and other auxiliary equipment. The RPB was packed with Teflon mesh, which serve as the packing material enhancing the contact between the gas and liquid phase. The RPB dimensions and the range of experimental conditions are shown in Table 1. The influences of high gravity factor ($\beta$) were estimated using the high gravity field strength, $r\omega^2/g$, where $g$ is gravity acceleration, and r and $\omega$ represent the average radius and rotational velocity of the RPB rotator, respectively. The volume of the RPB absorption column is estimated using $\pi(r_1^2 - r_2^2)Z_B$, where $r_1$, $r_2$, and $Z_B$ represent the outer radius, inner radius, and axial height of the packed bed rotator, respectively.

### 2.2 Experimental Procedure

The $H_2S$ bearing gas drawn by blower from copper smelting contaminated acid tank after drying and metering is allowed to enter from the outer edge to center of the rotating packed bed, while the sodium hydroxide solution was sprayed from center to the outer edge of the rotating packed bed. Gas–liquid phase flowed in the opposite direction forming a countercurrent packed bed rotator. The concentration of $H_2S$ was measured by online hydrogen sulfide analyzer.

The contaminated acids are stored in a tank having dimension of 6 m diameter, height of 8 m. The liberation of $H_2S$ was initiated by charging a dose of $Na_2S$. Sufficient time was allowed for the reaction to complete and to generate sufficient quantity of $H_2S$ at known concentration. The concentration of $H_2S$ was estimated using the online $H_2S$ analyzer. A constant concentration and flow rate of $H_2S$ release from the acid tank were ensured throughout the duration of single experiment.

The removal efficiency of $H_2S$ in the rotating packed bed is defined as

$$E = \frac{C_1 - C_0}{C_1} \times 100\% \tag{1}$$

where $E$ is the removal efficiency of $H_2S$, $C_1$ and $C_0$ are the concentrations of $H_2S$ in inlet and outlet gas streams, respectively.

The experimental overall volumetric gas side mass transfer coefficient ($K_Ga$) of the rotating packed bed is evaluated using the equation given below [24]

$$k_Ga = \frac{-Q_G}{\pi\left(r_1^2 - r_2^2\right)Z_B}\ln\left[1 - E\right] \tag{2}$$

where, $Q_G$ represent the volumetric flow rate of gas, and $E$ is the removal efficiency of $H_2S$, respectively.

## 3 Results and Discussion

### 3.1 Effect of High Gravity Factor on Removal Efficiency of $H_2S$

Figures 2 and 3 show the dependence of removal efficiency of $H_2S$ ($E$) and overall volumetric gas side mass transfer coefficient ($K_Ga$) with high gravity factor for two different gas flow rates. An increase in the high gravity factor was found to increase with the $E$ and $K_Ga$. The rate of increase was higher until high gravity factor of 60, while beyond was found to reach an asymptote. An increase in high gravity factor could possibly provide smaller liquid droplet, a thinner liquid film,

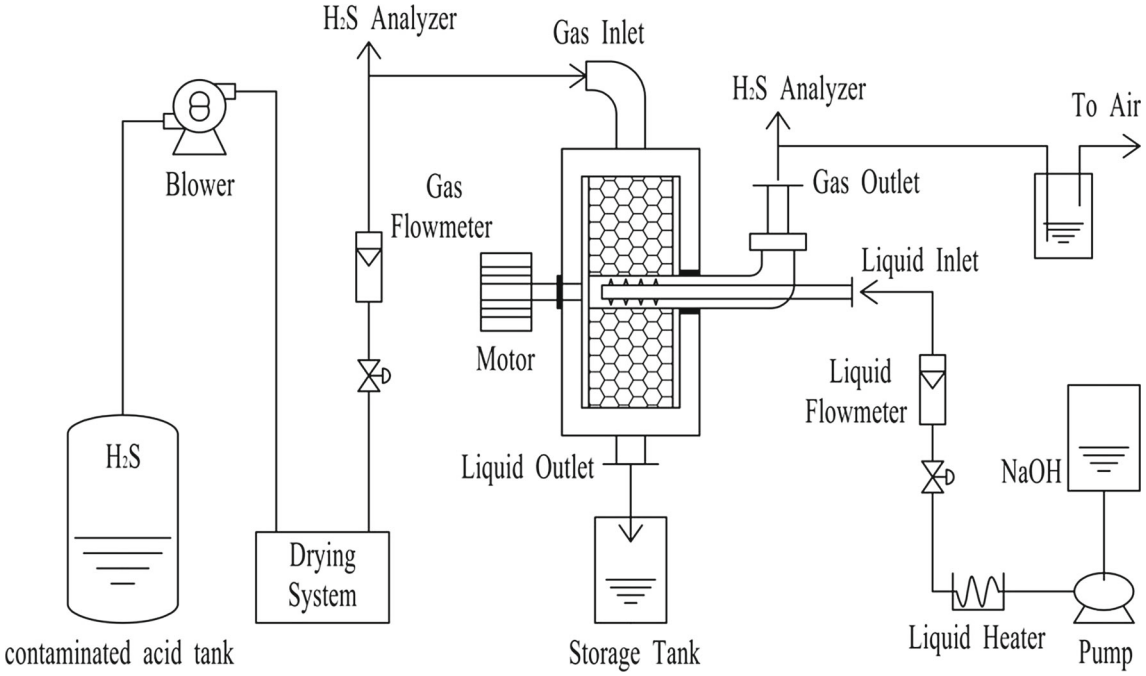


**Fig. 1** Scheme of experimental setup

**Table 1** Design and operating conditions of packed bed and rotating packed bed

| Items | Units | RPB |
|---|---|---|
| Inner radius of the packed bed ($r_2$) | m | 0.02 |
| Outer radius of the packed bed ($r_1$) | m | 0.115 |
| Average radius of the packed bed ($r_{avg}$) | m | 0.0675 |
| Axial height of the packed bed ($Z_B$) | m | 0.045 |
| Volume of the packed bed ($V_B$) | $m^3$ | 0.00181 |
| Specific area of packing per unit volume of a packed bed ($a_p$) | $m^2/m^3$ | 960 |
| Porosity ($\varepsilon$) | | 92% |
| Rotational speed | rpm | 300–1200 |
| The influences of high gravity factor ($\beta$) | | 6.66–106.6 |
| absorbent temperature ($T$) | K | 293–333 |
| concentration of sodium hydroxide ($C_{NaOH}$) | mol/L | 0.3–1.5 |
| mass concentration of $H_2S$ in feed gas ($C_{H2S}$) | $mg/m^3$ | 500–3000 |
| Gas flow rate ($Q_G$) | $m^3/h$ | 1–11 |
| Liquid flow rate ($Q_L$) | L/h | 10–70 |
| $Q_G/Q_L$ ratio | | 18–300 |

and diffusion depth, contributing to an enhancement in the mass transfer rate. However, on the other hand an increase in the high gravity factor would reduce the residence time of the phases that would reduce the mass transfer rate. The effect of increase in mass transfer rate due to gravity factor was offset by the decrease in the mass transfer rate due to the reduction in residence time results in an asymptote beyond the critical gravity factor. Considering the high absorption efficiency, the optimal gravitational factor can be considered as 80.

### 3.2 Effect of $Q_G$ on Removal Efficiency of $H_2S$

Figures 4 and 5 present the dependences of removal efficiency of $H_2S$ ($E$) and overall volumetric gas side mass transfer coefficient ($K_Ga$) on the gas flow rate for two gravity factors. An increase in the gas flow rate was found to decrease $E$ while the $K_Ga$ was found to increase. An increase in the gas flow rate is expected to increase the mass transfer rate (reduced mass transfer resistance) on account of better

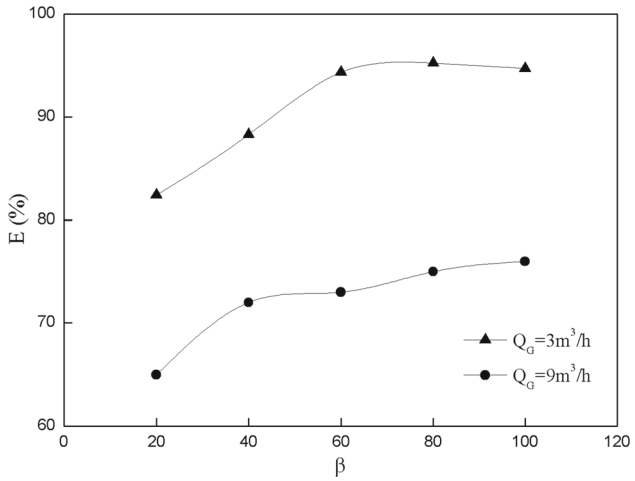


**Fig. 2** Removal efficiency of $H_2S$ at varied $\beta$

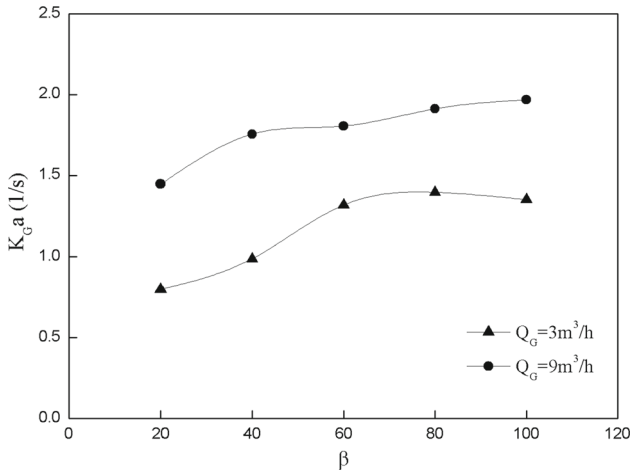


**Fig. 3** Overall volumetric gas side mass transfer coefficient at varied $\beta$ [$C_1$: 1500 mg/m$^3$, $Q_L$: 55 L/h, $C_{NaOH}$: 1.2 mol/L and $T$: 298 K]

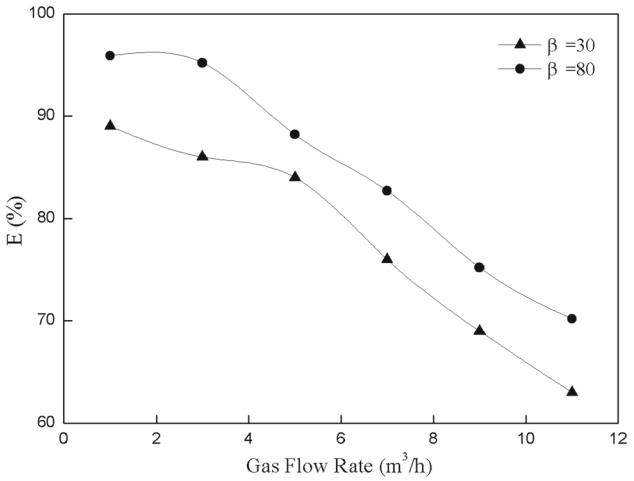


**Fig. 4** Removal efficiency of $H_2S$ at varied gas flow rate

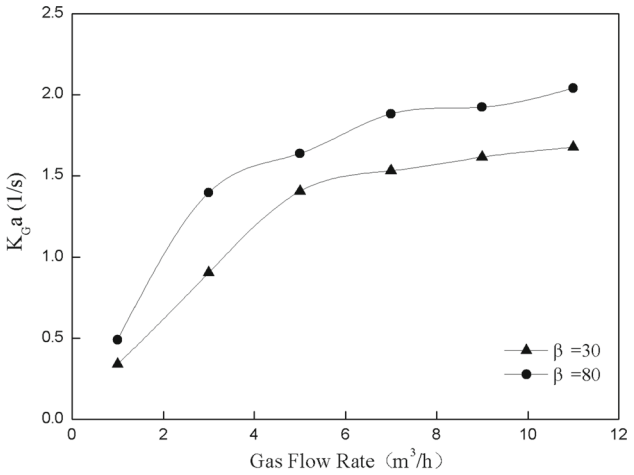


**Fig. 5** Overall volumetric gas side mass transfer coefficient at varied gas flow rate: [$H_2S$ concentration of 1500 mg/m$^3$, $Q_L$ of 55 L/h, sodium hydroxide concentration of 1.2 mol/L and absorbent temperature of 298 K

turbulence (Reynolds number) while a reduction in $E$ could be attributed to the combined effect of increase load and reduction in the residence time of the phased due to high mass flow rate. The rate of $K_Ga$ increase is faster at low gas flow rates while it was slower at higher gas flow rates. This again could be attributed to the relative magnitude of the two opposing effects discussed above. The relative magnitude of $Q$ and $E$ in Eq. 2 governs the rate of increase of $K_Ga$. Based on the high absorption efficiency at lower gas flow rates, a gas flow rate of 3 m$^3$/h can be considered optimal.

### 3.3 Effect of $Q_L$ on Removal Efficiency of $H_2S$

Figures 6 and 7 show the dependence of removal efficiency of $H_2S$ ($E$) and overall volumetric gas side mass transfer coefficient ($K_Ga$) on $Q_L$ for two different gravity factors. An increase in the liquid flow rate was found to increase $E$ and $K_Ga$. An increase in the liquid flow rate is expected to reduce the liquid phase mass transfer resistance due to faster surface renewal contributing to an increase in the gas absorption. The higher gas absorption is reflected with an increase in the $K_Ga$. Although the absorption efficiency increased due to decrease in liquid phase resistance, the concentration of the liquid leaving the absorption system could be lower demanding higher energy for regeneration. Considering the high absorption efficiency, the optimal liquid flow rate can be considered as 55 L/h.

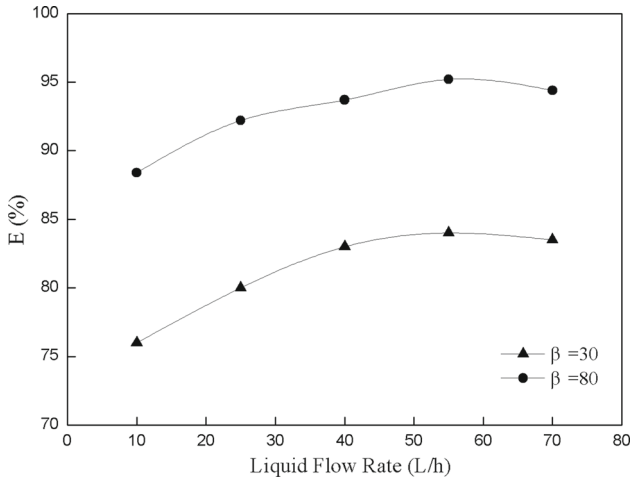


**Fig. 6** Removal efficiency of $H_2S$ at varied liquid flow rate

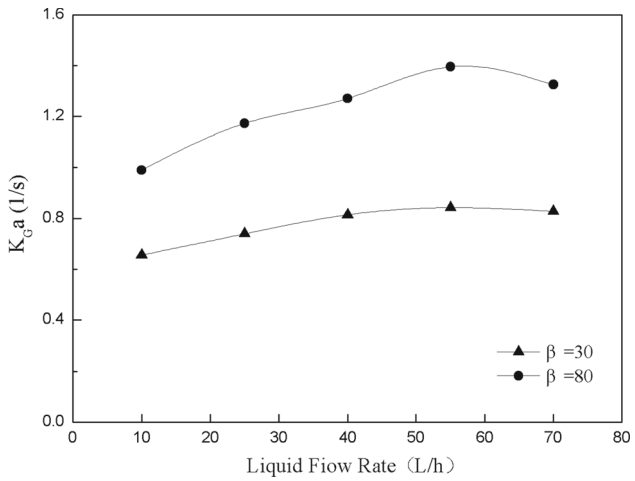


**Fig. 7** Overall volumetric gas side mass transfer coefficient at varied liquid flow rate: $H_2S$ concentration of 1500 mg/m$^3$, $Q_G$ of 3 m$^3$/h, sodium hydroxide concentration of 1.2 mol/L, and absorbent temperature of 298 K

## 3.4 Effect of Sodium Hydroxide Concentration on Removal Efficiency of $H_2S$

Figures 8 and 9 show the dependence of removal efficiency of $H_2S$ ($E$) and overall volumetric gas side mass transfer coefficient ($K_Ga$) on sodium hydroxide concentration at two different liquid flow rates. An increase in the NaOH concentration is found to increase in $E$ and $K_Ga$, attaining a maximum at concentration of 1.2 mol/L. An increase in the concentration of the absorbent (NaOH) is expected to increase in the liquid phase concentration driving force and hence a higher liquid phase transfer rate. An increased liquid side transfer rate contributes to an increase in the gas phase absorption efficiency and mass transfer coefficient. Considering the increase $E$ and $K_Ga$ attaining a maximum at 1.2 mol/l, it can be considered as the optimal liquid phase concentration.

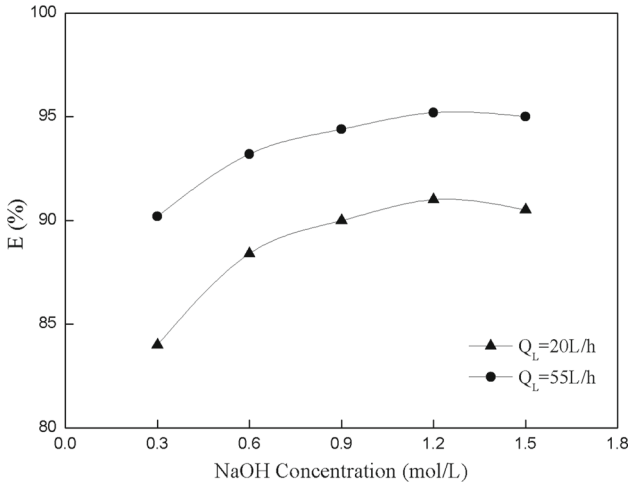


**Fig. 8** Removal efficiency of $H_2S$ at varied NaOH concentration

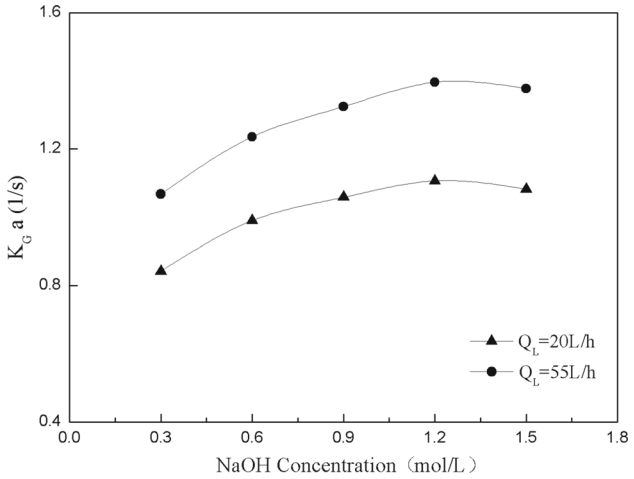


**Fig. 9** Overall volumetric gas side mass transfer coefficient at varied NaOH concentration: high gravity factor of 80, $H_2S$ concentration of 1500 mg/m$^3$, $Q_G$ of 3 m$^3$/h and absorbent temperature of 298 K

## 3.5 Effect of $H_2$ S Concentration on Removal Efficiency of $H_2S$

Figures 10 and 11 display the dependence of removal efficiency of $H_2S$ ($E$) and overall volumetric gas side mass transfer coefficient ($K_Ga$) with $H_2S$ concentration at two different NaOH liquid flow rates. An increase in the $H_2S$ concentration is found to decrease $E$ as well as $K_Ga$. The reduction in absorption efficiency with increase in the concentration of $H_2S$ seems to contract the basic principles of mass transfer from outlook. An increase in the concentration of absorbate is expected to increase the concentration driving force and hence should contribute to an overall increase in the transfer rate. Although the $\%E$ decreases, an over-

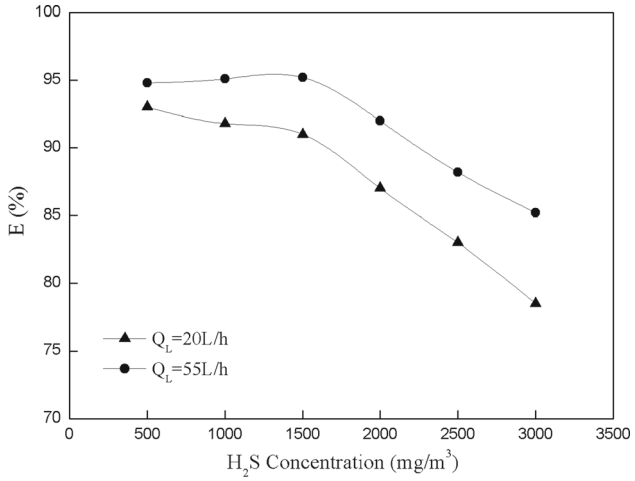


**Fig. 10** Removal efficiency of $H_2S$ at varied $H_2S$ concentration

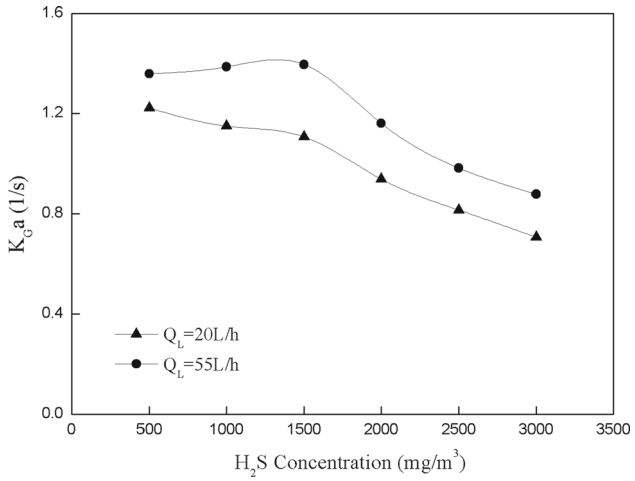


**Fig. 11** Overall volumetric gas side mass transfer coefficient at varied $H_2S$ concentration: high gravity factor of 80, NaOH concentration of 1.2 mol/L, $Q_G$ of 3 $m^3$/h and absorbent temperature of 298 K

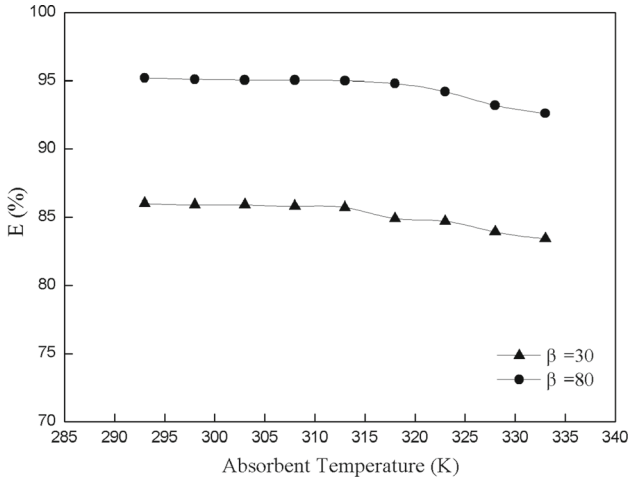


**Fig. 12** Removal efficiency of $H_2S$ at varied solution temperature

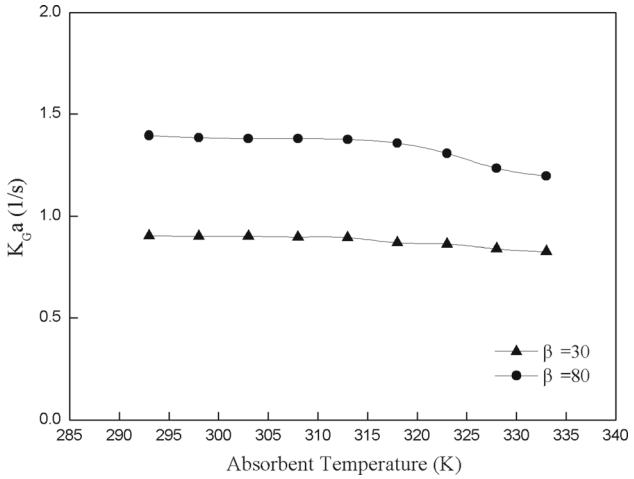


**Fig. 13** Overall volumetric gas side mass transfer coefficient at varied solution temperature: $H_2S$ concentration of 1500 mg/$m^3$, NaOH concentration of 1.2 mol/h, $Q_G$ of 3 $m^3$/h and $Q_L$ of 55 L/h

all mass balance clearly indicates the transfer rates increase with increase in the $H_2S$ concentration. For example, the net amount of $H_2S$ transferred is about 2400 mg of $H_2S$ at an initial concentration of 3000 mg/$m^3$ as compared to 1350 mg at an initial concentration of 1500 mg/$m^3$, although the $\%E$ is 80% for initial concentration of 3000 mg/$m^3$ while it is 90% for an initial concentration of 1500 mg/$m^3$. The definition of $K_Ga$ is such it depends on $\%E$ and gas flow rate which reflect the trend of $\%E$.

## 3.6 Effect of Absorbent Temperature on Removal Efficiency of $H_2S$

Figures 12 and 13 exhibit the dependence of removal efficiency of $H_2S$ ($E$) and overall volumetric gas side mass transfer coefficient ($K_Ga$) on absorbent temperature at two different gravity factors. An increase in the absorbent temperature is not found to significantly affect $E$ $K_Ga$. An increase in the temperature of absorbent is expected to increase the transfer rates on the one hand due to higher diffusional rates, and favorable physical properties while on the other hand would reduce the solubility of absorbate in the absorbent. The effects contradict each other result in insignificant effect on the absorption efficiency and the gas phase mass transfer coefficient.

## 3.7 Comparison of Rotating Packed Bed and Traditional Tower

Attempt was made to assess the effectiveness of the RPB absorption system in comparison with the conventional packed bed absorbers. The comparison of the equipment dimensions and operating parameters is provided in Table 2. A comparison of the $E$ and $K_Ga$ in the rotating packed bed

**Table 2** Comparison of mass transfer between rotating packed bed and traditional tower

| Items | Packed tower | RPB |
|---|---|---|
| Inner radius of a packed bed ($r_2$), m | | 0.02 |
| Outer radius of a packed bed ($r_1$), m | 0.75 | 0.115 |
| Axial height of a packed bed ($Z_B$), m | 4 | 0.045 |
| Volume of a packed bed, $m^3$ | 7.069 | 0.00181 |
| Specific area of packing per unit volume of a packed bed | 2400 | 960 |
| Absorbent temperature, K | 298 | 298 |
| High gravity factor | | 80 |
| $H_2S$ concentration, $mg/m^3$ | 1500 | 1500 |
| NaOH concentration, mol/L | 1.2 | 1.2 |
| Gas flow rate, $m^3/h$ | 600 | 3 |
| Liquid flow rate, L/h | 12,000 | 55 |
| $Q_G/Q_L$ ratio | 50 | 54.5 |
| $E$ | 86% | 95.2% |
| $K_Ga$, 1/s | $4.6 \times 10^{-2}$ | 1.4 |

and a conventional packed was made at similar $Q_G/Q_L$ ratio, ensuring similarity of throughput. The removal efficiency of $H_2S$ for the RPB was found to be higher by 10% while the $K_Ga$ was found to be 30 times higher. Additionally it should be noted that the conventional packed dimension is several orders of magnitude higher than the RPB, requiring far higher capital cost while the RPB would demand an increased operating cost due to the generation of high gravity factor. The literature shows that RPB has the advantages of high mass transfer efficiency, small equipment footprint and low running cost [25–27].

The rate of mass transfer between gas and liquid in RPB is 1–3 orders of magnitude larger than that of conventional method, resulting in a dramatic reduction of reaction time. RPB is also regarded as an ideal reactor since it is able to greatly intensify micromixing of fluids, and the rate of mass transfer in a RPB is much larger than that of traditional methods[28–30]. Therefore, the profits of RPB are much higher.

## 4 Conclusions

The removal of $H_2S$ from copper smelting contaminated acid using sodium hydroxide (NaOH) as absorbent was investigated in a RPB reactor. The major conclusion can be summarized as follows:

1. $K_Ga$ increased with increase in high gravity factor, absorbent and absorbate flow rate and concentration of sodium hydroxide while decreased with increase in mass concentration of $H_2S$ in feed gas.
2. $E$ increased with increase in high gravity factor, flow rate and concentration of sodium hydroxide while decreased with increase in flow rate and mass concentration of $H_2S$ in feed gas.
3. The increase in the temperature of absorption did not show any significant effect on $E$ and $K_Ga$.
4. The $K_Ga$ in the rotating packed bed reactor was about 30 times higher than the conventional packed bed at similar gas liquid throughputs.
5. $H_2S$ removal efficiency is about 95.2% which could be achieved at a gravity factor of 80, gas flow rate of $3\,m^3/h^1$, liquid flow ratio of 55 L/h, concentration of sodium hydroxide of 1.2 mol/L, mass concentration of $H_2S$ lower than $1500\,mg/m^3$, at a temperature of 298 K.

**Acknowledgements** This work was supported by National Natural Science Foundation of China (51604135).

## References

1. Krouse, H.R.; Viau, C.A.; Eliuk, L.S.; Ueda, A.; Halas, S.: Chemical and isotopic evidence of thermochemical sulphate reduction by light hydrocarbon gases in deep carbonate reservoirs. Nature **333**(6172), 415–419 (1988)
2. Qian, Z.; Xu, L.B.; Li, Z.H.; Li, H.; Guo, K.: Selective absorption of $H_2S$ from a gas mixture with $CO_2$ by aqueous N-methyldiethanolamine in a rotating packed bed. Ind. Eng. Chem. Res. **49**(13), 6196–6203 (2010)
3. Yi, F.; Zou, H.K.; Chu, G.W.; Shao, L.; Chen, J.F.: Modeling and experimental studies on absorption of $CO_2$ by benfield solution in rotating packed bed. Chem. Eng. J. **145**(3), 377–384 (2009)
4. Guo, K.; Zhang, Z.Z.; Luo, H.J.; Dang, J.X.; Qian, Z.: An innovative approach of the effective mass transfer area in the rotating packed bed. Ind. Eng. Chem. Res. **53**(10), 4052–4058 (2014)
5. Subham, P.; Aloke, K.G.; Bishnupada, M.: Theoretical studies on separation of $CO_2$ by single and blended aqueous alkanolamine solvents in flat sheet membrane contactor (FSMC). Chem. Eng. J. **144**(3), 352–360 (2008)

6. Li, J.L.; Chen, B.H.: Review of $CO_2$ absorption using chemical solvents in hollow fiber membrane contactors. Sep. Purif. Technol. **41**(2), 109–122 (2005)
7. Niu, H.; Pan, L.; Su, H.; Wang, S.: Effects of design and operating parameters on $CO_2$ absorption in microchannel contactors. Ind. Eng. Chem. Res. **48**(18), 8629–8634 (2009)
8. Clarke, E.T.; Solouki, T.; Russell, D.H.: Transformation of polysulfidic sulfur to elemental sulfur in a chelated iron, hydrogen sulfide oxidation process. Anal. Chim. Acta **299**(1), 97–111 (1994)
9. Mcmanus, D.; Martell, A.E.: The evolution, chemistry and applications of chelated iron hydrogen sulfide removal and oxidation processes. J. Mol. Catal. A Chem. **117**(1), 289–297 (1997)
10. Eng, S.J.; Motekaitis, R.J.; Martell, A.E.: The effect of end-group substitutions and use of a mixed solvent system on β-diketones and their iron complexes. Inorg. Chim. Acta. **278**(2), 170–177 (1998)
11. Eng, S.J.; Motekaitis, R.J.; Martell, A.E.: Degradation of coordinated β-diketonates as iron chelate catalysts during the oxidation of $H_2S$ to $S_8$ by molecular oxygen. Inorg. Chim. Acta. **299**(1), 9–15 (2000)
12. Piche, S.; Ribiero, N.; Bacaoui, A.: Assessment of a redox alkaline/iron-chelate absorption process for the removal of dilute hydrogen sulfide in air emissions. Chem. Eng. Sci. **60**(22), 6452–6461 (2005)
13. Kelleher, T.; Fair, J.R.: Distillation studies in a high-gravity contactor. Ind. Eng. Chem. Res. **35**(12), 4646–4655 (1996)
14. Ramshaw, C.: Higee distillation—an example of process intensification. Chem. Eng. **389**(389), 13–14 (1983)
15. Ramshaw, C.; Mallinson, RH.: Mass Transfer Process. ed: Google Patents (1981)
16. Ramshaw, C.: The opportunities for exploiting centrifugal fields. Heat Recovery Syst. CHP **13**(13), 493–513 (1993)
17. Lin, C.C.; Ho, T.J.; Liu, W.T.: Distillation in a rotating packed bed. J. Chem. Eng. Jpn. **35**(12), 98–1304 (2002)
18. Chen, Y.S.; Liu, H.S.: Absorption of VOCs in a rotating packed bed. Ind. Eng. Chem. Res. **41**(6), 1583–1588 (2002)
19. Sun, B.C.; Wang, X.M.; Chen, J.M.: Simultaneous absorption of $CO_2$ and $NH_3$ into water in a Rotating Packed Bed. Ind. Eng. Chem. Res. **48**(24), 11175–11180 (2009)
20. Lin, C.C.; Chao, C.Y.; Liu, M.Y.; Lee, Y.L.: Feasibility of ozone absorption by $H_2O_2$ solution in rotating packed beds. J. Hazard. Mater. **167**(13), 1014–1020 (2009)
21. Lin, C.C.; Liu, W.T.: Ozone oxidation in a rotating packed bed. J. Chem. Technol. Biotechnol. **78**(78), 138–141 (2003)
22. Chen, J.F.; Wang, Y.H.; Guo, F.; Wang, X.M.; Zheng, C.: Synthesis of nanoparticles with novel technology: high-gravity reactive precipitation. Ind. Eng. Chem. Res. **39**(4), 948–954 (2000)
23. Lin, C.C.; Liu, W.T.: Removal of an undesired component from a valuable product using a rotating packed bed. J. Ind. Eng. Chem. **12**(3), 455–459 (2006)
24. Lin, C.C.; Liu, W.T.: Mass transfer characteristics of a high-voidage rotating packed bed. J. Ind. Eng. Chem. **13**(1), 71–78 (2007)
25. Xu, J.; Liu, C.; Wang, M.: Rotating packed bed reactor for enzymatic synthesis of biodiesel. Bioresour. Technol. **224**, 292–297 (2017)
26. Li, W.; Song, B.; Li, X.: Modelling of vacuum distillation in a rotating packed bed by Aspen. Appl. Therm. Eng. **117**, 322–329 (2017)
27. Modak, J.B.; Bhowal, A.; Datta, S.: Extraction of dye from aqueous solution in rotating packed bed. J. Hazard. Mater. **304**, 337–342 (2016)
28. Yang, H.J.; Chu, G.W.; Zhang, J.W.; Shen, Z.G.; Chen, J.F.: Micromixing efficiency in a rotating packed bed: experiments and simulation. Ind. Eng. Chem. Res. **44**(20), 7730–7737 (2005)
29. Chen, J.; Zheng, C.; Chen, G.A.: Interaction of macro- and micromixing on particle size distribution in reactive precipitation. Chem. Eng. Sci. **51**(10), 1957–1966 (1996)
30. Chen, J.F.; Gao, H.; Zou, H.K.: Cationic polymerization in rotating packed bed reactor: experimental and modeling. Aiche J. **56**(4), 1053–1062 (2010)